Rare Metal Materials and Engineering
Volume 49, Issue 9, September 2020
Available online at www.rmme.ac.cn

Science Press

Cite this article as: Rare Metal Materials and Engineering, 2020, 49(9): 2948-2955.

ARTICLE

Effect of $Ce(SO_4)_2$ Concentration on Properties of Ni-W-Ce Alloy Coating Prepared by Jet-electrodeposition

Fu Xiuqing, Wang Qingqing, Lin Jinran, Shen Moqi, Xu Ye

Nanjing Agricultural University, Nanjing 210031, China

Abstract: In order to investigate the relationship between $Ce(SO_4)_2$ concentration and surface performance, a series of workpieces coated with Ni-W-Ce alloy were fabricated by jet-electrodeposition. The cellular structure was observed by SEM, and the composition of coating was analyzed by EDS. XRD analysis shows that the coating has lattice distortion. LEXT4100 laser confocal microscope was used to observe wear mark and it is found that the friction mechanism changes. The results indicate that the addition of $Ce(SO_4)_2$ improves the surface micromorphology of the coating, and the best surface quality appears when the concentration is 0.5 g/L. Meanwhile, the micro-hardness, wear resistance and corrosion resistance show a rule of first getting better and then getting worse with increasing the concentration. When the concentration of $Ce(SO_4)_2$ is 0.5 g/L, the micro-hardness reaches the peak value of 5196.9 MPa, and the wear resistance is the best, with the wear resistance parameters dropping to the valley value. The corrosion resistance is also the best with the corrosion potential of −0.5537 V, and the arc reactance radius is the minimum.

Key words: jet-electrodeposition; $Ce(SO_4)_2$; Ni-W-Ce alloy coating; wear resistance; corrosion resistance

Nowadays, it is difficult for mechanical parts to meet the high operating requirements. Corrosion failure and abrasion failure are the main causes for parts failure. Improving the surface performance of parts can extend the parts' service life, improve the use stability of instruments and reduce the cost of enterprises. Preparing coatings on the surface of workpieces is one of the most common methods to change surface properties[1-3]. As a common surface engineering, jet-electrodeposition has been widely used in mechanical, aerospace and electronic fields due to its high efficiency, easy management and selectivity [4-6]. In recent years, the nickel-based coating has attracted attention of many scholars. Some up to date studies report that the surface performance can be significantly improved by adding W, Co, and other elements [7-9]. W is very popular because of its melting point, boiling point, hardness, corrosion resistance. Scholars found that Ni-W alloy coating can improve the hardness and corrosion resistance of nickel-based coating [10-12].

Rare earth elements have chemically active properties for their special atomic structure. They are widely used in electronics, machinery, energy, environmental protection, agriculture and other fields. The addition of rare earth elements will improve the surface properties of the coating. Its influence is mainly manifested in the following aspects: deposition rate, surface morphology, wear resistance, corrosion resistance, etc [13,14]. Zhang et al[15] prepared Ni-W alloy coating by electrodeposition and found that rare earth doping can effectively improve the hardness and wear resistance of the coating. Du et al[16] found that the corrosion potential of Ni-P-PTFE composite coating with lanthanum rare earth element moves up by 300 mV, the impedance value increases nearly three times, and the corrosion resistance is significantly improved.

Ce, a rare earth element, plays a catalytic role in many reactions, because of its unique oxidation property. Ce becomes an important object to study the properties of rare earth elements[17-19]. In the deposition process, Ce^{4+} can adsorb the defect of the coating, improve the surface morphology and performance of the coating, and thus extend the service life of the workpiece.

Received date: September 13, 2019
Foundation item: China Postdoctoral Science Foundation (2017M621665); Postdoctoral Science Foundation of Jiangsu Province of China (2018K022A); Postgraduate Research & Practice Innovate Program of Jiangsu Province (SJCX19_0145)

Corresponding author: Fu Xiuqing, Ph. D., Associate Professor, College of Engineering, Nanjing Agricultural University, Nanjing 210031, P. R. China, Tel: 0086-25-58606580, E-mail: fuxiuqing@njau.edu.cn

Previous researches have largely focused on the improvement of coating properties after adding rare earth elements, while the coatings were prepared by chemical plating and electrodeposition, and less by jet-electrodeposition[20]. In order to expand the application of rare earth elements in jet-electrodeposition, the influence of $Ce(SO_4)_2$ concentration on micro-hardness, wear resistance and corrosion resistance of jet-electrodeposition Ni-W-Ce alloy coating was studied.

1 Experiment

1.1 Preparation of alloy coating

#45 steel cubic workpiece (25 mm×10 mm×8 mm) was used as the basis material. The plating solution composition is shown in Table 1. All reagents were analytical reagent with deionized water. Before jet-electrodeposition, the workpiece was polished step by step with abrasive paper of 320#, 800# and 1500#, and then activated. The main steps of activating process are follows: oil removal → weak activation → strong activation

After the activation, the workpiece was placed in the jet-electrodeposition plating device. Nickel rod was used as the anode to ensure the concentration of Ni^{2+}. The processing parameters adopted are shown in Table 2.

1.2 Methods for analysis and testing of coatings

A field emission scanning electron microscope (FEI-SEM, Quanta FEG 250; FEI Instruments, OR, USA) was used to characterize the surface morphology. Energy dispersive spectroscopy (EDS) from X-ray diffraction and elemental analysis system (XFlash Detector 5030, Bruker AXS, Berlin, Germany) were applied to measure the content of the element. The micro-hardness was measured by holding a 100 g load for 15 s with the help of a micro-hardness measurement instrument (Duramin-40, Struers, Denmark) and five replicates were averaged. The phase analysis was carried out by a full set of X-ray diffractometer-spectrometer (PANalytical X-ray Diffractometer Model X'pert Powder; PANalytical Inc., Holland). The CFT-Ⅰ material surface comprehensive performance tester was used to detect the surface wear resistance. During the test, the coating surface was scratched back and forth for 20 min with a grinding ball. The wear mark was 4 mm long and the mass of grinding ball was 320 g with a reciprocating speed of 500 T/min. The parameters (width, depth, and cross-sectional area) of wear marks on the coating surface were measured by an OLYMPUS LEXT4100 laser confocal microscope. The three-pole electrochemical workstation (CS350) was used to measure the polarization curve and impedance spectrum and to analyze the electrochemical corrosion behavior. The corrosion medium was 50 g/L NaCl solution.

2 Results and Discussion

2.1 Analysis of the micromorphology of coating surface

The surface micromorphology of Ni-W-Ce alloy coatings with different concentrations of $Ce(SO_4)_2$ is shown in Fig.1.

A typical cellular structure is obviously presented on the coating surface, which strictly follows the two-dimensional crystal core growth model.

Fig.1a shows the morphology of Ni-W alloy coating, whose cellular structure is clear and compact, and the size distribution is uneven. Furthermore, the coating has defects, like obvious pits and bumps. Fig.1b~1d show the micromorphologies of the surface after adding $Ce(SO_4)_2$ into plating solution. With the increase of Ce^{4+} concentration, the average size of the cellular structure is enlarged and the distribution becomes regular. And the coating surface tends to be flat. When the concentration of $Ce(SO_4)_2$ reaches 0.5 g/L, thick cellular structure is deposited on the coating surface, which is so thick that no holes and defects form. Due to the good absorbability of Ce^{4+}, the reaction products prefer to be absorbed on the surface defects. With the growth of the cellular structure, the surface becomes smoother and performs better. As shown in Fig.1e, when the concentration of $Ce(SO_4)_2$ is 0.7 g/L, the plating solution contains a large number of Ce^{4+}. The increase of free metal ion concentration results in large amounts of heterogeneous deposition, thus leading to an uneven size distribution.

The composition of the alloy coating is analyzed by EDS. Element distribution of the coating and its counterparts are shown in Fig.1f~1j and Table 3. Ni, W and Ce elements are detected in the coating, indicating the successful preparation of the Ni-W-Ce alloy coating. According to the Table, the Ce element content increases with the augment of the $Ce(SO_4)_2$ concentration. It also affects the content of

Table 1 Composition of plating solution

Component	Concentration/$g\cdot L^{-1}$
$NiSO_4\cdot 6H_2O$	40
$Na_2WO_4\cdot 2H_2O$	30
$C_6H_8O_7$ (citric acid)	80
CH_4N_2S (thiourea)	0.01
$C_{12}H_{25}SO_4Na$ (sodium dodecyl sulfate)	0.08
$Ce(SO_4)_2$	0.1~0.7

Table 2 Optimal jet-electrodeposition experimental parameters

Parameter	Value
Current/A	0.4
Temperature/°C	50
Processing time/min	20
pH value	1.0~1.5

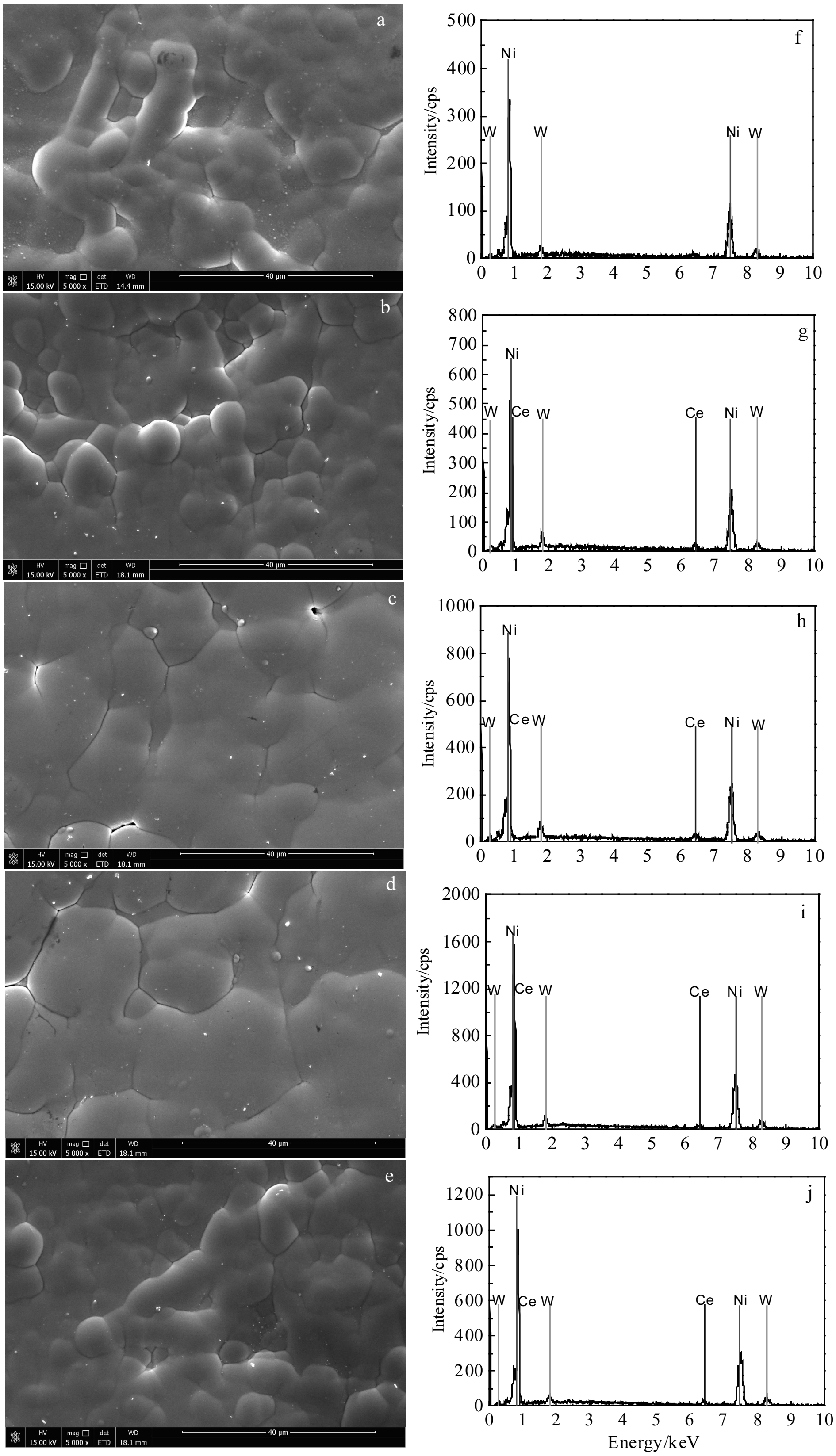

Fig.1 Surface micromorphologies (a~e) and EDS spectra (f~j) of Ni-W alloy coatings with different concentrations of Ce(SO_4)$_2$: (a, f) 0 g/L, (b, g) 0.1 g/L, (c, h) 0.3 g/L, (d, i) 0.5 g/L, and (e, j) 0.7 g/L

Table 3 Composition of the alloy coating with different concentrations of $Ce(SO_4)_2$ (at%)

Element	$Ce(SO_4)_2$ concentration/g·L^{-1}				
	0	0.1	0.3	0.5	0.7
Ni	87.71	88.44	88.51	88.87	84.76
W	14.29	10.02	8.77	7.96	11.02
Ce	0.00	1.54	2.72	3.17	4.22

other elements, because Ce, which is a third secondary group element, is specific stable tetravalent. Ce can accelerate the movement of charge, thus increasing the deposition rate of the coating. This is the reason for the increase of Ni content in the coating. However, W cannot be deposited in the coating alone, and must be co-deposited with Ni^{2+}. Due to the cathode reduction of Ni^{2+} is promoted, less Ni^{2+} is available for co-deposition. The rate of co-deposition reaction is relatively slow, resulting in a relatively small average content of W element in the coating. When a large amount of Ce^{4+} is adsorbed on the surface of the coating, the potential range of the plating solution increases, inhibiting the reduction reaction of Ni^{2+}. The co-deposition of WO_4^{2-} and Ni^{2+} increases as the content of W increases in the alloy coating.

2.2 XRD phase analysis of coating

Fig.2 presents XRD patterns of Ni-W-Ce alloy coatings. XRD peaks at $2\theta=44°$ and $2\theta=51°$ correspond to Ni (111) and (200) crystal faces, respectively. According to Fig.2b, compared with Ni-W alloy coating, the position of the two diffraction peaks shifts to the left, indicating that lattice distortion occurs. Meanwhile, the bottom of the diffraction peak becomes wider and wider after adding $Ce(SO_4)_2$, indicating that $Ce(SO_4)_2$ can promote the flattening of the diffraction peak. Because of the low content of Ce in the coating (<5%), the XRD diffraction pattern cannot be detected.

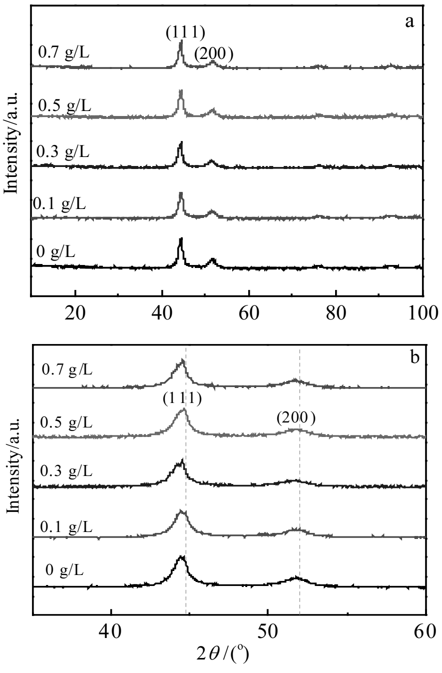

Fig.2 XRD patterns of Ni-W-Ce alloy coatings with different concentrations of $Ce(SO_4)_2$

2.3 Analysis of micro-hardness of the composite coating

The micro-hardness of #45 steel is 1473.6 MPa. Fig.3 shows results of micro-hardness measurements of Ni-W-Ce coatings, and coating micro-hardness increases with addition of $Ce(SO_4)_2$. When the concentration of $Ce(SO_4)_2$ reaches 0.5 g/L, micro-hardness reaches the peak value of 5196.9 MPa, which is ~27.63% higher than that of the Ni-W alloy coating (4072.0 MPa). However, when the concentration of $Ce(SO_4)_2$ reaches 0.7 g/L, the micro-hardness of coating decreases to 4379.0 MPa.

There are three reasons for the micro-hardness increase of Ni-W-Ce alloy coating. Firstly, Ce is highly adsorptive for its unique four valences. It can improve micro-hardness by reducing defects of coating. Secondly, due to the rare earth pinning effect, atoms exert agglomeration effect at the boundary. It can effectively resist dislocation movement under external force, so the coating micro-hardness is improved. Finally, Ce make the surrounding Ni-W crystal lattice distorted, resulting in the improvement of the micro-hardness of the alloy coating. However, when Ce^{4+} is excessive in the plating solution, it will cause greater cathode polarization. Meanwhile, the deposition of ions is hindered and uneven deposition occurs, which reduces the micro-hardness of the coating.

2.4 Analysis of wear resistance of coatings

According to the previous micro-hardness test results, it can be confirmed that the micro-hardness of the grinding ball is greater than that of the coating, which belongs to hard friction. The GCr15 grinding ball is used in this test, and the grinding ball can be pressed into the coating, forming wear mark as the coating surface experiences plastic deformation. In this work, the wear resistance of the composite coating is measured by the width, depth, cross-sectional area of wear mark and friction mechanism, observed by OLYMPUS LEXT4100 laser confocal microscope. Fig.4 shows the morphologies of wear marks, and the data are shown in Table 4.

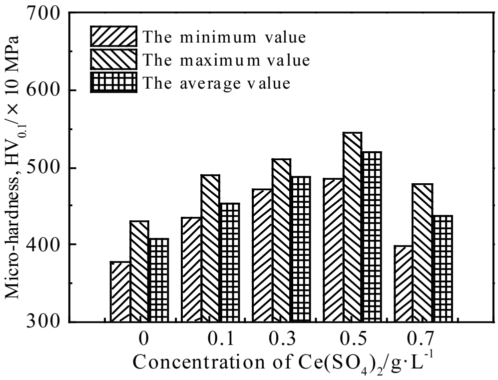

Fig.3 Micro-hardness of coatings with different concentrations of $Ce(SO_4)_2$

It can be seen from Fig.4 and Table 3 that the Ni-W alloy coating has the largest wear mark width, depth and area, indicating the worst wear resistance. The data of the surface wear trace morphology of the coating show a trend of decreasing first and then increasing with the increase of the concentration of $Ce(SO_4)_2$. When the concentration of $Ce(SO_4)_2$ reaches 0.5 g/L, the values of the wear mark width, depth and area are the minimum, and the wear amount is the smallest with the same length. The results show that the wear resistance of Ni-W alloy coating will improve with the addition of Ce. When the concentration of $Ce(SO_4)_2$ reaches 0.7 g/L, all the morphology parameters show an increasing trend, indicating that excessive concentration of $Ce(SO_4)_2$ will damage the improvement of the wear resistance of the coating. With the addition of $Ce(SO_4)_2$, Ce is evenly distributed in the coating. Due to the good wear resistance of Ce, it forms a wear-resistant framework. In addition, the existence of Ce causes lattice distortion and produces obvious nailing effect. Both of them cause the improvement of wear resistance. However, when the concentration of $Ce(SO_4)_2$ exceeds a certain limit, the uneven deposition of ions will cause stress concentration of alloy coating, resulting in reduced wear resistance.

From the perspective of friction mechanism, Fig.5 shows the micromorphologies of wear marks. It can be seen from Fig.5 that there are some pits, cracks and high-temperature oxidation generated on the surface of Ni-W alloy coating, which are determined by many factors. Firstly, the heat from friction softens the coating. Adhesive wear occurs between the coating and the grinding ball, making surface to peel off. And there is combination of abrasive wear and adhesive wear on the surface of Ni-W alloy coating. Secondly, when pressing the grinding ball, the coating plastic deformation occurs, producing local hardening and crack. Lastly, friction produces a lot of heat, Ni element in the alloy coating turns into Ni oxide at high temperature and oxygen in the joint. At initial stage, oxide as a lubricant can effectively protect the alloy coating. Over time, a large number of surface oxides are reduced, which causes secondary damage to the alloy coating. Ni-W-Ce alloy coating has a few of pits and high-temperature oxidation, and tiny furrow appears on the surface of wear marks, indicating that with the addition of $Ce(SO_4)_2$, rare earth phase compounds have obvious positive pinning effect on the alloy coating, which effectively improves the wear resistance of the coating, and the wear pattern turns into single abrasive wear. With the increase of the concentration, the furrow of wear marks gradually becomes shallower. Moreover, when the concentration of $Ce(SO_4)_2$ reaches 0.5 g/L, the coating surface shows slight scratches without

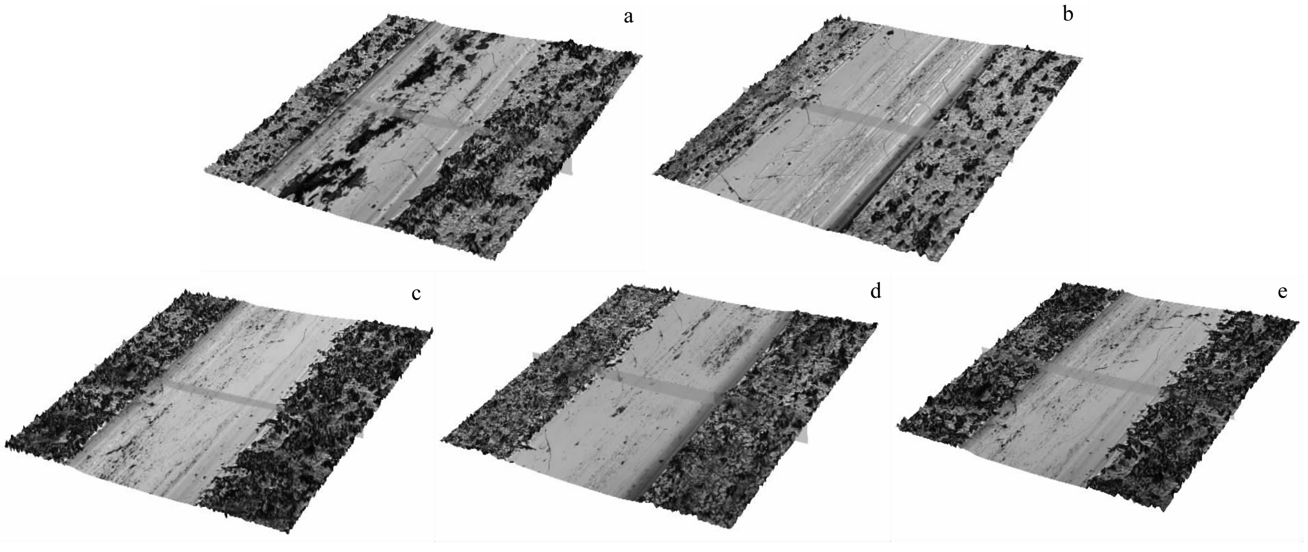

Fig.4 Wear mark morphologies of Ni-W coating with different concentrations of $Ce(SO_4)_2$: (a) 0 g/L, (b) 0.1 g/L, (c) 0.3 g/L, (d) 0.5 g/L, and (e) 0.7 g/L

Table 4 Wear mark parameters of Ni-W-Ce alloy coating with different concentrations of $Ce(SO_4)_2$

Concentration/g·L^{-1}	Width/μm	Depth/μm	Scratch area/μm^2
0	610.205	11.083	5098.258
0.1	574.999	10.551	4448.941
0.3	556.470	9.736	3980.897
0.5	541.647	8.303	3674.507
0.7	576.852	9.848	4117.493

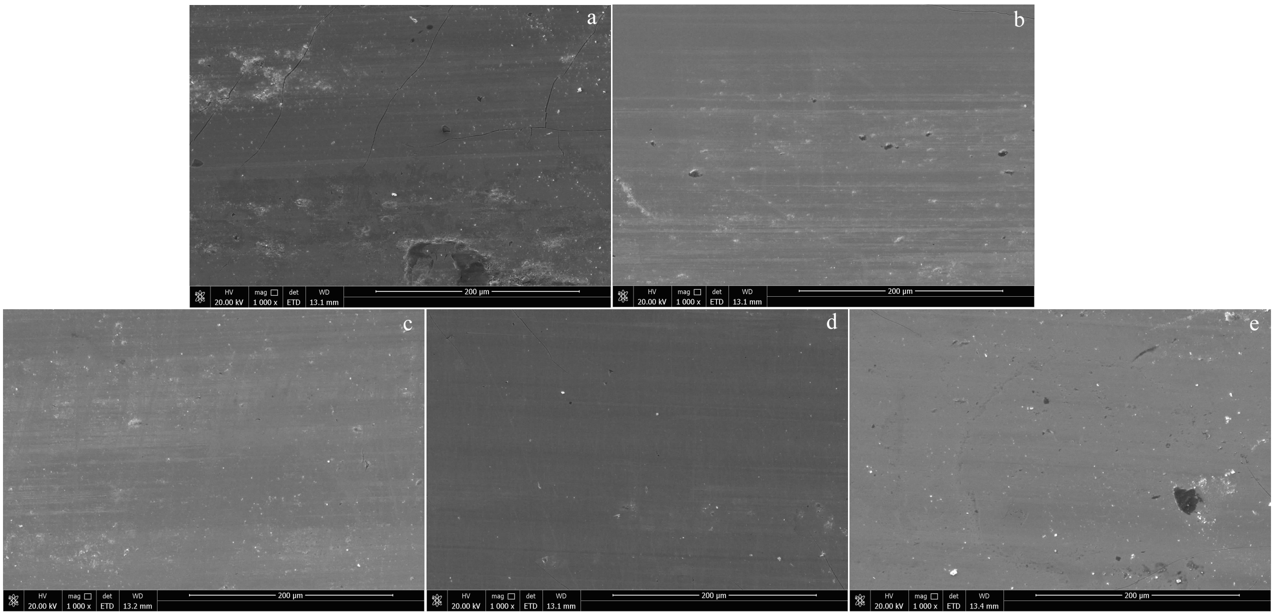

Fig.5 Micromorphologies of scratches of Ni-W coating with different concentrations of $Ce(SO_4)_2$: (a) 0 g/L, (b) 0.1 g/L, (c) 0.3 g/L, (d) 0.5 g/L, and (e) 0.7 g/L

obvious furrows. The reason for this phenomenon is that Ce has strong chemical activity and low melting point on the friction surface. In the process of friction, it melts to lubricate with heating. Besides, the napping effect of Ce greatly improves the micro-hardness of the coating. According to the classical Archard Law, under the same test conditions, the wear properties of the coating are in direct proportion to its hardness, and the increase of micro-hardness is conducive to the improvement of the friction and wear properties of the coating [21].

2.5 Analysis of corrosion resistance of coating

Coating corrosion resistance is obtained by a three-electrode electrochemical platform. Tafel curves are shown in Fig.6. Corrosion potential (E_{corr}) and current density (I_{corr}) are obtained from polarization curve epitaxy are shown in Table 5, B_a is the anode polarization slope and B_c is the cathode polarization slope. It can be seen that E_{corr} and I_{corr} of Ni-W alloy coating are −1.0324 V and 6.7027×10^{-5} A·cm^{-2}. The corrosion potential moves to 0 V. The corrosion current decreases with the addition of $Ce(SO_4)_2$, indicating that the corrosion resistance of the coating is improved. Moreover, it reaches the best when the concentration of $Ce(SO_4)_2$ is 0.5 g/L, and the E_{corr} and I_{corr} drop to −0.5537 V and 5.1936×10^{-6} A·cm^{-2}. while the E_{corr} and I_{corr} increase when the concentration of $Ce(SO_4)_2$ reaches 0.7 g/L, demonstrating that the corrosion resistance of the coating is worse, but still better than that of Ni-W alloy coating.

Fig.7 shows the Nyquist plots, and the values of parameters fitted by the equivalent circuit diagram are shown in Table 6. R_s is the resistance in solution, R_p is the charge transfer resistance; CPE is the constant phase angle element, and its impedance is follows:

$$Z=1/Y_0(j\omega)^{-n} \tag{1}$$

In the above formula, Y_0 is a constant, its dimensional for $\Omega^{-1}\cdot cm^{-2}\cdot s^{-n}$. n is a dimensionless parameter. If n=1, the CPE is an ideal capacitance. If n=0, the CPE is a pure resistance. However, n is between 0 and 1 in the actual solution.

As shown in Fig.7, the arc reactance radius of Ni-W-Ce alloy coating is greater than that of Ni-W alloy coating. It indicates that the AC impedance of the coating in the process of polarization increases after adding $Ce(SO_4)_2$ into the plating solution, and the corrosion resistance is enhanced. According to the data in Table 6, Ce can reduce the

Table 5 Corrosion parameters of Ni-W coating with different concentrations of $Ce(SO_4)_2$

Concentration/g·L^{-1}	B_a/mV	B_c/mV	I_{corr}/×10^{-5} A·cm^{-2}	E_{corr}/V	Corrosion rate/mm·a^{-1}
0	213.65	265.31	6.7027	−1.0324	0.811 26
0.1	431.15	269.09	3.4460	−0.8234	0.417 08
0.3	529.8	236.89	1.6641	−0.7572	0.2014
0.5	688.97	242.23	0.519 36	−0.5537	0.062 86
0.7	388.78	259.92	2.1228	−0.7897	0.256 93

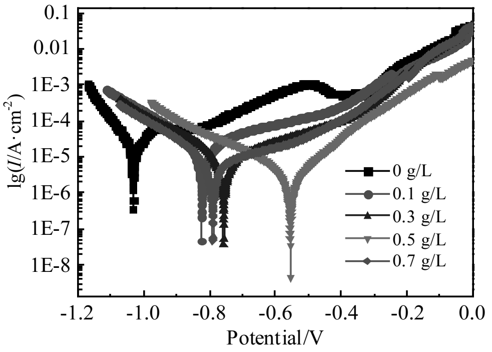

Fig.6 Polarization curves of coating with different concentrations of $Ce(SO_4)_2$

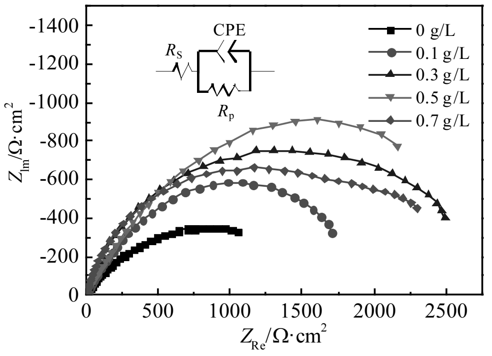

Fig.7 AC impedance spectra of coatings with different concentrations of $Ce(SO_4)_2$

polarization resistance R_p of the coating. The corrosion tendency of Ni-W-Ce alloy coating in NaCl solution is lower than that of Ni-W alloy coating. In addition, the charge transfer resistance is the largest, which is calculated by Zview software. It indicates that the charge is greatly hindered between the electrode and the solution, and the corrosion process is slow. To sum up, the corrosion resistance of coating will improve with the addition of $Ce(SO_4)_2$. The reasons are as follows. On the one hand, due to the nailing effect and adsorption of the rare earth Ce, the coating is flat and has few defects. It is difficult for corrosive medium to enter the coating, so as to improve the corrosion resistance of the coating. On the other hand, too much Ce^{4+} causes the large potential difference between the anode and the cathode. It inhibits the deposition of other ions and makes the coating performance worse.

Table 6 Equivalent circuit diagram parameter value under different concentrations of $Ce(SO_4)_2$

Concentration/g·L^{-1}	R_s/Ω·cm^2	CPE-T/×10^{-4} F·cm^{-2}	CPE-P	R_p/Ω·cm^2
0	2.717	5.7405	0.565 83	1313
0.1	3.289	4.5045	0.642 52	1925
0.3	2.182	1.4775	0.677 63	2655
0.5	3.289	4.5045	0.642 52	2860
0.7	2.952	1.3009	0.7077	2338

3 Conclusions

1) Ni-W-Ce alloy coating prepared by jet-electrodeposition has a typical cellular structure. When the concentration is 0.5 g/L, it has the best performance, including large cellular structure, smooth surface and a small number of defects. Furthermore, since Ce appears in the coating, the lattice distortion occurs in the alloy coating.

2) Compared to the Ni-W alloy coating, Ni-W-Ce alloy coating remarkably improves coating micro-hardness and the wear resistance. As the concentration of $Ce(SO_4)_2$ increases, both of them increase first and then decrease. When the concentration reaches 0.5 g/L, the micro-hardness of Ni-W-Ce alloy coating reaches the peak value of 5196.9 MPa, which is ~27.63% higher than that of Ni-W alloy coating. Meanwhile, the wear resistance of Ni-W-Ce alloy coating is also the best, and wear mark parameters (width, depth, and cross-sectional area) drop to the valley value.

3) Compared to the Ni-W alloy coating, Ni-W-Ce alloy coating also improves coating corrosion resistance. Corrosion potential of the Ni-W alloy coating is −1.0324 V. As the concentration of $Ce(SO_4)_2$ increases, the corrosion

resistance of the alloy coating increases first and then decreases. When the concentration reaches 0.5 g/L, the corrosion potential of the Ni-W-Ce alloy coating is −0.5537 V and the arc reactance radius is the minimum.

References

1 Wei Wenshuo, Song Zhaoxia, Zeng Seng *et al. Materials Science and Technology*[J], 2008, 26(5): 47 (in Chinese)

2 Tu Mingjing, Ou Zhongwen. *China Surface Engineering*[J], 2012, 25(5): 1 (in Chinese)

3 Xu Binshi, Ma Shining, Liu Shican *et al. Journal of Tongji University*, *Natural Science*[J], 2001(9): 1085 (in Chinese)

4 Fan Hui, Liu Man, Zhao Yangpei *et al. Key Engineering Materials*[J], 2018, 764: 164

5 Li Hengzheng, Kang Min, Zhang Yin *et al. China Surface Engineering*[J], 2018, 31(2): 103 (in Chinese)

6 Jiang Wei , Shen Lida, Qiu Mingbo *et al. Journal of Alloys and Compounds* [J], 2018, 762: 115

7 Li Baosong, Zhang Wen, Huang Yuxing *et al. Rare Metal Materials and Engineering*[J], 2008, 47(5): 1509

8 Hasanpour P, Salehikahrizsangi P, Raeissi K *et al. Surface & Coatings Technology*[J], 2019, 368: 147

9 Feng Shangbin, Jia Lina, Zhang Huarui *et al. Rare Metal Materials and Engineering*[J], 2019, 48(4): 1087

10 Ma Beilei, Wang Ruihong. *Corrosion and Protection*[J], 2019, 40(2): 116 (in Chinese)

11 Sun Fuyang, Zhao Guoxian, Guo Qingchao *et al. Surface Technology*[J], 2014, 43(6): 6 (in Chinese)

12 Jiang Kun, Lu Jianshu. *Material Protection*[J], 2008, 51(7): 63 (in Chinese)

13 Zhou Shuzheng, Shen Chengjin, Han Shaoguang *et al. Materials Research Express*[J], 2019, 6(8): 1

14 Wang Chunyu, Li Huanran, Zhang Peng *et al. Journal of Materials Engineering and Performance*[J], 2013, 22(2): 624

15 Zhang Xuehui, Chen Hao, Li Xiaoxian *et al. Rare Metal Materials and Engineering*[J], 2016, 45(10): 2605

16 Du Baozhong, Wang Bo, Lu Leilei. *Rare Metal Materials and Engineering*[J], 2011, 40(S2): 229

17 Zhang Guangyao, Wang Chenglei, Gao Yuan *et al. Rare Metal Materials and Engineering*[J], 2015, 44(5): 1229

18 Pang Qiu, Hu Zhili, Zhang Rong *et al. Rare Metal Materials and Engineering*[J], 2016, 45(7): 1826

19 Yi Huan, Cai Shuizhou, Zou Hui. *Rare Metal Materials and Engineering*[J], 2018, 47(4): 1185

20 Yang Zijian, Fu Chuanqi, Wang Zhou *et al. Surface Technology*[J], 2019, 48(2): 99 (in Chinese)

21 Xue Yujun, Si Donghong, Liu Hongbin *et al. The Chinese Journal of Nonferrous Metals*[J], 2011, 21(9): 2157 (in Chinese)

$Ce(SO_4)_2$浓度对电喷镀 Ni-W-Ce 合金镀层性能影响

傅秀清，王清清，林尽染，沈莫奇，徐 烨

（南京农业大学，江苏 南京 210031）

摘 要：为了研究 $Ce(SO_4)_2$浓度与合金镀层表面性能的关系，采用电喷镀制备了一系列 Ni-W-Ce 合金镀层工件。用扫描电镜(SEM)观察了镀层的表面结构，并用能谱仪(EDS)检测镀层中的元素组成。用 XRD 分析镀层的物相组织，表明 $Ce(SO_4)_2$加入后镀层发生晶格畸变。使用 CFT-Ⅰ型材料表面综合性能测试仪在镀层表面进行磨痕制备，并通过 LEXT4100 激光共焦显微镜和 SEM 观察磨痕形貌，表征镀层耐磨性和磨损机理。结果表明，添加 $Ce(SO_4)_2$改善了涂层的表面微观形貌，当其浓度为 0.5 g/L 时，涂层的表面质量最佳。同时，显微硬度、耐磨性和耐腐蚀性随浓度的增加呈现先好后坏的规律。当 $Ce(SO_4)_2$浓度为 0.5 g/L 时，镀层显微硬度、耐磨性和耐腐蚀性均取得最佳，此时的显微硬度数值达到峰值 5196.9 MPa，其耐磨性表征参数均取得最小值，且腐蚀电位为−0.5537 V，电弧电抗半径最小。

关键词：电喷镀；$Ce(SO_4)_2$；Ni-W-Ce 合金镀层；耐磨性；耐蚀性

作者简介：傅秀清，男，1981 年生，博士，副教授，南京农业大学工学院，江苏 南京 210031，电话：025-58606580，E-mail：fuxiuqing@njau.edu.cn